Med Biol Eng Comput (2016) 54:1553–1562
DOI 10.1007/s11517-015-1434-0

ORIGINAL ARTICLE

Surface deformation and reaction force estimation of liver tissue based on a novel nonlinear mass–spring–damper viscoelastic model

Árpád Takács[1] · Imre J. Rudas[1] · Tamás Haidegger[1,2]

Received: 21 September 2015 / Accepted: 11 December 2015 / Published online: 30 December 2015

Abstract Rheological soft tissue models play an important role in designing control methods for modern teleoperation systems. In the meanwhile, these models are also essential for creating a realistic virtual environment for surgical training. The implementation of model-based control in teleoperation has been a frequently discussed topic in the past decades, offering solutions for the loss of stability caused by time delay, which is one of the major issues in long-distance force control. In this paper, mass–spring–damper soft tissue models are investigated, showing that the widely used linear models do not represent realistic behavior under surgical manipulations. A novel, nonlinear model is proposed, where mechanical parameters are estimated using curve fitting methods. Theoretical reaction force curves are estimated using the proposed model, and the results are verified using measurement results from uniaxial indentation. The model is extended with force estimation by nonuniform surface deformation, where the surface deformation function is approximated according to visual data. Results show that using the proposed nonlinear model, a good estimation of reaction force can be achieved within the range of 0–4 mm, provided that the tissue deformation shape function is appropriately approximated.

Tamás Haidegger is a Bolyai Fellow of the Hungarian Academy of Sciences. This work has been supported by ACMIT (Austrian Center for Medical Innovation and Technology), which is funded within the scope of the COMET (Competence Centers for Excellent Technologies) program of the Austrian Government.

✉ Árpád Takács
arpad.takacs@irob.uni-obuda.hu

[1] ABC-iROB, Óbuda University, Budapest, Hungary

[2] Austrian Center for Medical Innovation and Technology (ACMIT), Wiener Neustadt, Austria

Keywords Soft tissue modeling · Robotic tissue palpation · Tissue parameter estimation

1 Introduction

In the past years, research activities related to robotic surgery have gained much attention due to the rapid development of interventional systems [7]. Cutting, indentation and grabbing are just a few types of tissue manipulations that require high-precision tools and techniques. In order to achieve better performance for surgical robotics applications in terms of stable control for teleoperation, it is crucial to understand the behavior of soft tissues through their mechanical properties [6]. Creating an accurate tool–tissue interaction model would largely aid the design of model-based control methods. This way, force response of the manipulation is estimated using the model, and the required input force (control signal) can be calculated that would control the tissue holder (in most cases, the robotic arm) in order to carry out the surgical manipulation tasks in an efficient, stable and accurate way. A comprehensive study of the existing tool–tissue interaction models was presented by Famaey and Sloten in [5], collecting these into 3 major categories:

- *Continuum mechanics-based* models, which are mostly based on finite element analysis approaches;
- *Heuristic* models, which are built up from linear or nonlinear basic mechanical elements such as springs and dampers;
- *Hybrid* models, which usually represent a combination of the above-mentioned approaches [13].

- It is widely accepted that continuum mechanics-based models provide the most realistic response functions.

However, a significant disadvantage of this approach is the vast computational requirement, limiting their usability in real-time simulations and applications. The heuristic models, which are also often referred to as the mass–spring–damper models or rheological models, are very popular in modeling surgical manipulation tasks, mainly indentation and grabbing [12]. Using heuristic models, analytical solutions could be provided, making this a great advantage of using this approach in many modeling aspects of tool–tissue interaction [17]. Several works provide measurement data for soft tissue indentation force response in both relaxation [15] and compression phases [2]. Heuristic models were comprehensively discussed by Yamamoto, comparing several simple models in point-to-point palpation for detecting hidden lumps in soft tissues [21]. Alkhouli et al. investigated the mechanical properties of human adipose tissues, although the linear viscoelastic model they used was only applied in the stress relaxation phase [1]. Troyer et al. [18] created a nonlinear viscoelastic model that was validated with relaxation tests, which is implementable in finite element algorithms in order to decrease computational requirements. These models, along with the appropriate image guidance and modeling, can largely increase the accuracy and safety of surgical interventions [14]. Mechanical models can also be integrated with visual cues in order to improve the performance of haptic feedback devices. Such virtual models were used in pseudo-haptic feedback-based methods by Li et al. [10] using a silicone phantom tissue with embedded hard incisions. A complex tissue model was presented by Leong et al. [8] where some of the soft tissue parameters were integrated, although the correct acquisition of the parameters was not successful. Some relevant measurement results were still published [9], despite the ill-formed mathematical description.

In their paper, the surface deformation shape was estimated to be exponential, although this assumption was not supported by any literature or experimental reference, and the relevant geometrical parameters were not published, either. The resulting transfer function was incorrectly derived for the proposed model, which resulted in an estimated force response with no physical meaning. Consequently, the published parameters were not fit to the experimental data; therefore, the discussion of results was incomplete and incorrect. The paper was concluded by modifying the Dirac-delta function so that it would fit a single measurement point in the experimental results. To correct these shortcomings of the a priori research, this paper follows the same basic idea as Leong et al. then correctly deriving the mathematical formulae, and approximating tissue parameters and surface deformation shape, based on reproducible experimental data, which will be used for the verification of the proposed nonlinear soft tissue model.

2 Methods

2.1 Theoretical considerations

A detailed explanation of the structure of mass–spring–damper models has been published by Wang and Hirai, investigating the behavior of serial and parallel models [20]. They also discussed experimental results related to the rheological behavior of commercially available clay and Japanese sweets materials, using model parameter estimation. In this paper, the soft tissue model shown in Fig. 1 is used, like it was employed by Leong et al. [9]. This paper aims to follow their basic idea, using correct mathematical description. In this approach, there is a uniform distribution of Wiechert bodies under the surface of the soft tissue, creating a reaction force when the tissue surface is deformed. The total reaction force is calculated by adding up the force response values of each, infinitely small element, connected to a corresponding surface element. Their displacement is assumed to be known at any time. In the first part of this work, uniform surface deformation problems will be discussed in order to verify the proposed soft tissue model. After acquiring the mechanical parameters, the force response is estimated from an approximated, nonuniform deformation, as a verification of the complex approach. The unknown parameters of the model, such as the mechanical parameters of the spring and damper elements, are calculated from experimental data.

The mass–spring–damper modeling approach is a simple pragmatic way of modeling the behavior of soft tissues. Due to the unique material properties of soft tissues (anisotropy, viscoelasticity, inhomogeneity, etc.), describing their behavior under manipulation tasks is very different from other materials that are used in industrial or other service robotic applications. The main idea of this approach is that linear or nonlinear spring and damper elements are combined together in a serial or parallel way, creating an assembly, which, when subjected to deformation, would present similar mechanical properties as the

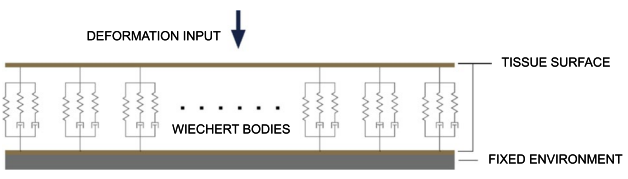

Fig. 1 The proposed linear tool–tissue interaction model, where the Wiechert bodies are distributed along the tissue surface

represented soft tissue. In most cases, these models are used for describing tissue behavior in the case of uniaxial elongation. However, early efforts have also been made to create models and devices for measuring rheological properties in biaxial elongation [4]. In order to efficiently apply this model, the $u(t)$ deformation paths of the end points of the combined mechanical elements need to be known in time. Provided that this information is given, the force response can be described with a simple mathematical expression. The reaction force arising in the mechanical elements can be determined from basic mechanical properties. In the case of a spring element, this force (f_s) is calculated from the spring stiffness value (k) and the deformation of the spring in the longitudinal direction. The reaction force (f_d) arising in the damper elements is calculated using the damping coefficient value (b) and the rate of deformation of the damper element. In heuristic soft tissue modeling, there are three basic models that are commonly used for describing tissue behavior in terms of viscoelasticity: the Kelvin–Voigt, the Maxwell and the Kelvin models, as shown in Fig. 2 [12].

The Kelvin–Voigt model is the most commonly used heuristic model in analytical mechanics, capable of representing stress relaxation and reversible deformation. There exists an analytical solution to the force response in the form of an ordinary differential equation. This model is very popular in many fields of study due to its simplicity and easy interpretation. However, step-input response functions cannot be modeled using the Kelvin–Voigt model, as the reaction force arising as a result of a step-like deformation would be infinitely large due to the parallel connection of the damper element. In the time domain, the force response function for the Kelvin–Voigt model is described by:

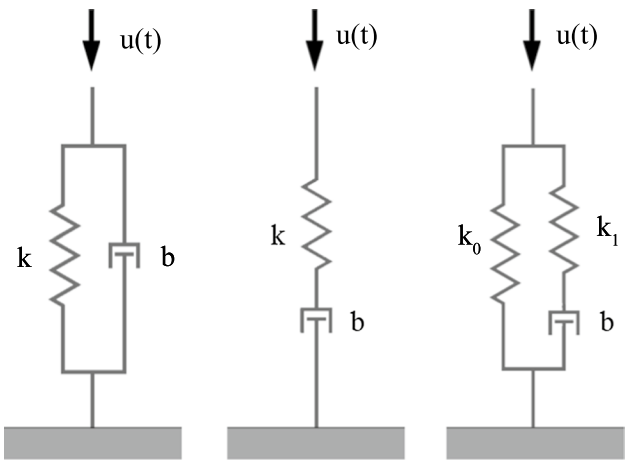

Fig. 2 Commonly used models for representing the mechanical behavior of viscoelastic materials: Kelvin–Voigt model (*left*), Maxwell model (*center*) and the Kelvin model (*right*)

$$f_{\mathrm{KV}}(t) = b\dot{u}(t) + ku(t), \tag{1}$$

where $u(t)$ is the deformation function. Similarly, the force response function in the frequency domain is as follows:

$$F_{\mathrm{KV}}(s) = (bs + k)U(s). \tag{2}$$

The Maxwell model is the simplest approach to model *creep*, the phenomenon of permanent deformation due to mechanical stresses. In this model, a damper and a spring element are connected serially, making the model usable for modeling stress relaxation. A major drawback of the Maxwell model is that the force response value (f_{M}) will asymptotically converge to 0 in the case of a constant deformation input. Therefore, this model is not capable of modeling residual stresses. The actual deformation of the system cannot be expressed as a function of the acting forces, which is the result of the internal dynamics of this model, since the position of the virtual mass point connecting the spring and damper elements cannot be measured. On the other hand, in the frequency domain, the transfer function can be easily determined:

$$F_{\mathrm{M}}(s) = \frac{kbs}{bs + k}U(s). \tag{3}$$

The Kelvin body is created by the parallel connection of a Maxwell element and a single linear spring element. This combination is often referred to as the Standard Linear Solid model in viscoelasticity, providing the simplest possible approach of representing residual stress, stress relaxation and elastic behavior in the case of step inputs. In the time domain, there exists a closed-form formulation, written as follows:

$$f_{\mathrm{K}}(t) + \frac{b}{k_1}\dot{f}_{\mathrm{K}}(t) = k_0\left(u(t) + \frac{b}{k_0}\left(1 + \frac{k_0}{k_1}\dot{u}(t)\right)\right). \tag{4}$$

In the frequency domain, the transfer function of the Kelvin element is:

$$F_{\mathrm{K}}(s) = \frac{b(k_0 + k_1)s + k_0k_1}{bs + k_1}U(s). \tag{5}$$

Due to the rapid development in the fields of robot control and surgical robotics, the creation of more sophisticated models has become essential in soft tissue behavior modeling. The accuracy requirements of advanced robotic surgical applications were not met anymore by the previously described simple models. In order to achieve better performance in these applications, new combinations of damper and spring elements were proposed. A new dynamic model is shown in Fig. 3, where Kelvin and Maxwell bodies are connected serially, creating a mass–spring–damper model consisting of five mechanical elements. The major advantages of this model are that both the elastic behavior and

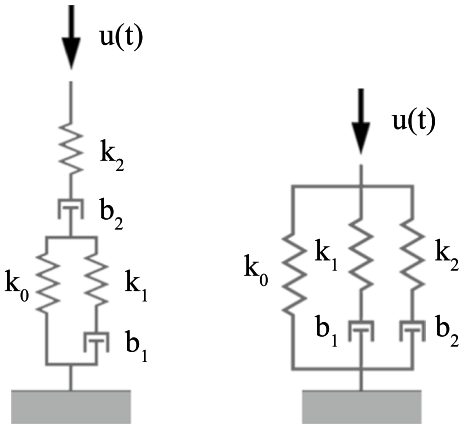

Fig. 3 Two basic combinations of the mass–spring–damper viscoelastic models: the Maxwell–Kelvin model (*left*) and the Wiechert model (*right*)

stress relaxation of the tissue can be described in a significantly more effective and sophisticated manner, compared to the general Kelvin model. In the frequency domain, the transfer function is written as:

$$F_{\mathrm{MK}}(s) = \frac{A_{2_{\mathrm{MK}}}s^2 + A_{1_{\mathrm{MK}}}s}{B_{2_{\mathrm{MK}}}s^2 + B_{1_{\mathrm{MK}}}s + B_{0_{\mathrm{MK}}}}U(s), \tag{6}$$

where $A_{2_{\mathrm{MK}}}, A_{1_{\mathrm{MK}}}, B_{2_{\mathrm{MK}}}, B_{1_{\mathrm{MK}}}, B_{0_{\mathrm{MK}}}$ are linear combinations of parameters k_0, k_1, k_2, b_1 and b_2. Increasing the complexity of a heuristic model does not necessarily lead to better accuracy in terms of system behavior modeling. In the case of the Maxwell–Kelvin, used in [8], the reaction force will converge to 0, similarly to the Maxwell model; therefore, this model is clearly not the best choice for modeling long-term stress relaxation. It can easily be seen that if there is any damper element that is placed in the "cross section" of the model (there is no spring element "bypassing" the flow of the force), the resulting steady-state reaction force would be 0.

If a Kelvin body and several Maxwell bodies are connected in a parallel way, the generalized Maxwell model is created. If there is only one Maxwell body integrated in the model, its simplest form, the Wiechert model, is derived. With this approach, the modeling of the reaction force becomes smooth and significantly more accurate due to the possibility of finer "tuning" of mechanical parameters. A detailed comparison between the standard linear solid and the Wiechert models has been provided by Wang et al. [19], highlighting the advantages of using the latter in liver and spleen organ force response modeling. Parameter estimation of the Wiechert model has also been done by Machiraju et al. [11], although the results were only based on tissue relaxation data, proposing its integration into finite element modeling software. The transfer function of the Wiechert model is as follows:

$$F_{\mathrm{W}}(s) = \frac{A_{2_{\mathrm{W}}}s^2 + A_{1_{\mathrm{W}}}s + A_{2_{\mathrm{W}}}}{B_{2_{\mathrm{W}}}s^2 + B_{1_{\mathrm{W}}}s + B_{0_{\mathrm{W}}}}U(s) = W_{\mathrm{W}}(s)U(s), \tag{7}$$

where

$$\begin{aligned}
A_{2_{\mathrm{W}}} &= b_1 b_2 (k_0 + k_1 + k_2),\\
A_{1_{\mathrm{W}}} &= (b_1 k_2 (k_0 + k1) + b_2 k_1 (k_0 + k_2),\\
A_{0_{\mathrm{W}}} &= k_0 k_1 k_2 b_2,\\
B_{2_{\mathrm{W}}} &= b_1 b_2,\\
B_{1_{\mathrm{W}}} &= b_1 k_2 + b_2 k_1,\\
B_{0_{\mathrm{W}}} &= k_1 k_2.
\end{aligned}$$

2.2 Experimental methods

In this work, the mass–spring–damper models distributed under the deformed tissue surface are represented by the Wiechert model (Fig. 1). The model parameters were obtained by applying a uniform deformation input on the surface during the following experiment. Six pieces of cubic-shaped fresh beef liver samples were investigated, with edge lengths of 20 ± 2 mm. The size of each specimen was measured before and after the experiments. Each of the specimens was compressed at three different compression rates: a slow rate of 20 mm/min, a medium rate of 100 mm/min and a near-step input at 750 mm/min (maximum compression rate provided by the system). The indentation tests were carried out at the Austrian Center for Medical Innovation and Technology (ACMIT), Wiener Neustadt, on a Thümler GmbH TH 2730 tensile testing machine connected to an Intel Core i5-4570 CPU with 4GB RAM, using the ZPM 251 (v4.5) software. The force response data were collected with an ATI Industrial Automation Nano 17 titanium six-axis Force/Torque transducer, using the 9105-IFPS-1 DAQ Interface and power supply at 62.5 Hz sampling time. An Intel Core i7-2700 CPU with 8 GB RAM hardware and the ATICombinedDAQFT .NET software interface was used for data visualization and storage. In the case of each specimen (marked by letters A–F), at first, the low- and medium-speed indentation tests were carried out, reaching 4 mm of indentation depth. The deformation input function was also recorded for validation purposes. A custom-made 3D-printed indenter head with a flat surface larger than the specimen surface size was mounted on the force transducer. The movement of the head started 1 mm above the specimen surface, and in the evaluation, only the first 3.6 mm of indentation data was used in order to filter out any nonlinearity in the ramp-input function. In the first two cases, data were recorded only during the head movement, while each specimen was subjected to indentation 12 times. The force response curves showed no

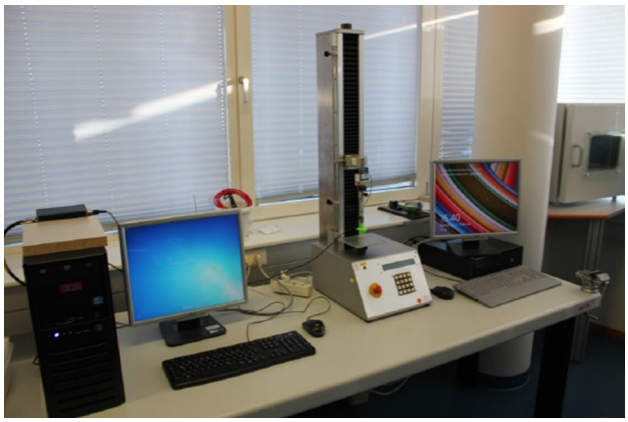

Fig. 4 Experimental setup for beef liver indentation tests at the Austrian Center for Medical Innovation and Technology (ACMIT)

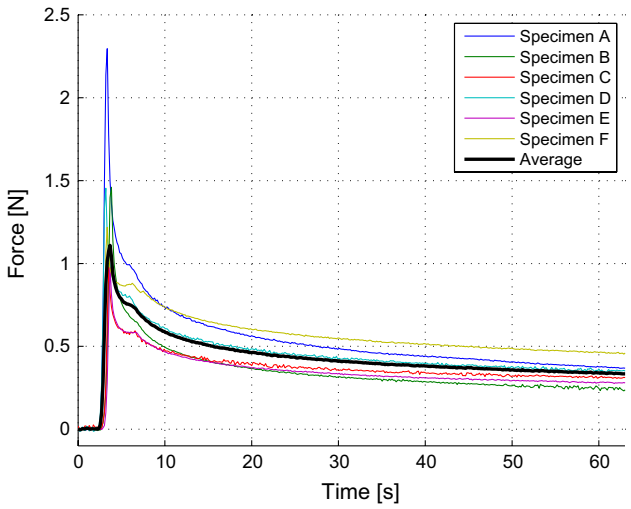

Fig. 5 Force response curves for step-input relaxation tests for 8 identically cut liver pieces

systematic deviation from the first responses, which allows one to assume that no substantial tissue damage was caused during the initial experiments. The final, near-step input was applied several times on each specimen, although it was found that the force response magnitude in the relaxation phase (1 min) decreased significantly during the second and third experiments on the same tissue, supposedly from the severe damage to the internal structure. Therefore, in the case of each specimen, only the very first set of measured data points was used for the parameter estimation from the force response relaxation data. A photograph of the experimental setup is shown in Fig. 4.

2.3 Indentations tests

In order to have an initial estimation on the soft tissue parameters, the force response data from relaxation tests were evaluated. The indentation speed of 750 mm/min was approximated with a step input. An analytical expression for the force response of the soft tissue can be easily calculated by obtaining the inverse Laplace transform of (7), using partial fraction decomposition, where the transfer function $W_W(s)$ is multiplied by the Laplace transform of the step-input function.

$$f_{\mathrm{W}r}(t) = \mathscr{L}^{-1}\left\{W_{\mathrm{W}}(s)\frac{x_d}{s}\right\} = x_d\left(k_0 + k_1\left(1 - e^{-\frac{k_1}{b_1}t}\right) + k_2\left(1 - e^{-\frac{k_2}{b_2}t}\right)\right), \tag{8}$$

where $f_{\mathrm{W}r}(t)$ is the force magnitude during the relaxation tests and $x_d = 4$ mm is the depth of the compression at the maximum deformation. The relaxation data for all six specimens are displayed in Fig. 5. For better visual representation, the average response curves are also shown in Fig. 5, which were obtained by taking the average values of the response data from each specimen, weighted with respect to its surface size and normalized to 20×20 mm. It is important to note that an unexpected break in the curves was observed in all cases, which is most likely the effect of the deceleration of the indenter, as it reaches the prescribed depth. In the authors' opinion, this break does not affect the force response results significantly, because the most relevant sections of the response curves are the initial relaxation slopes (force relaxation) and the steady-state values (residual stress). As the closed-form solution to the step input was given, curve fitting on the original measurement data was applied. For this procedure, the MATLAB *cftool* toolbox was used. The parameters were independently obtained for each of the six specimens and were compensated by the tissue surface magnitude, resulting in six sets of parameters of stiffness and damping values:

$$k_i^c = k_i\frac{A_0}{A} \quad i = 1,2,3 \tag{9}$$

$$b_j^c = b_j\frac{A_0}{A} \quad j = 1,2, \tag{10}$$

where A is the surface area of each specimen and $A_0 = 400\,\mathrm{mm}^2$ is the reference surface size. The average parameter values are listed in Table 1.

The Wiechert model gives a very good approximation of the soft tissue behavior in the force relaxation phase. To validate the results, two more sets of indentation tests with constant compression rates were carried out on each of the specimens, as was published in [16]. Utilizing the same method for obtaining the analytical force response as in the step-input case, the following analytical expression was obtained for the force response:

Table 1 Parameter estimation results from force relaxation and constant compression rate tests

Model Type	K_0 (N/m)	K_1 (N/m)	K_2 (N/m)	b_1 (Ns/m)	b_2 (Ns/m)	κ_0 (m^{-1})	κ_1 (m^{-1})	κ_2 (m^{-1})	RMSE Combined (N)
Linear	4.86	57.81	53.32	9987	10464	–	–	–	0.1865
Nonlinear	2.03	0.438	0.102	5073	39.24	909.9	1522	81.18	0.0206

$$f_{W_c}(t) = \mathscr{L}^{-1}\left\{W_W(s)\frac{v}{s^2}\right\} = v\left(k_0 t + b_1\left(1 - e^{-\frac{k_1}{b_1}t}\right) + b_2\left(1 - e^{-\frac{k_2}{b_2}t}\right)\right), \tag{11}$$

where v denotes the compression rate (20 or 100 mm/min) and f_{W_c} stands for the force response magnitude. Ideally, by substituting the model parameters into (11), the force response data should predict the measurement data. Considering that the 750 mm/min indentation was approximated as a step input, a minor compensation of the previously obtained parameters would still be needed. However, the constant compression rate indentation results showed that the shape of the analytical response curve largely differs from that of the measured response, clearly questioning the validity of the Wiechert model in this indentation phase. From the haptics application point of view, tissue behavior under constant compression rate is significantly more relevant than under relaxation. The average measurement data and the predicted response curves at the compression rate of 100 mm/min are shown in Fig. 6. The best fitting curve, assuming positive mechanical parameter values, is also displayed.

The measurement data and its major deviation from the estimated response imply that the reaction force magnitude under constant compression rates represents progressive stiffness characteristics instead of a linear one. This phenomenon may be caused by the complex mechanical structure of the liver tissue, which cannot be observed during step-response relaxation tests. According to the Wiechert model, one would expect a superposition of reaction forces of a linearly elastic element (k_0) and two Maxwell bodies that introduce damping (stress relaxation) into the system, which is well represented by the analytical solution.

In order to keep the current model as simple as possible, nonlinearities will be introduced through spring elements. To create such a model, some basic restrictions should be introduced, based on practical considerations:

$$k_i(x) \geq 0, \tag{12}$$

$$\frac{\mathrm{d}k_i(x)}{\mathrm{d}x} \geq 0, \tag{13}$$

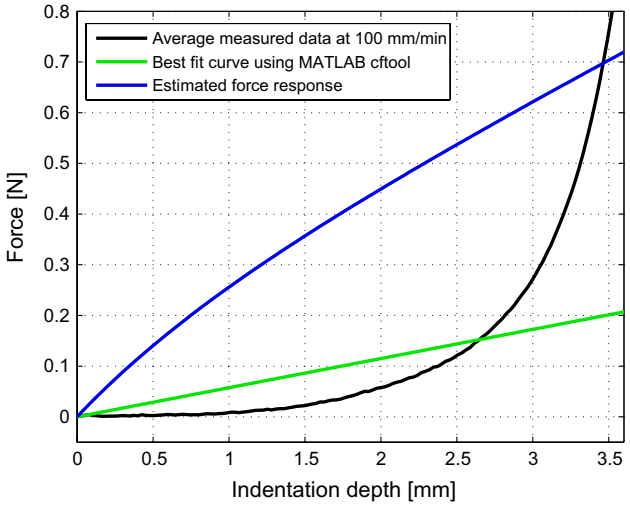

Fig. 6 Verification results of the linear Wiechert model at the compression rate of 100 mm/min. *The blue curve* shows the predicted force response from the parameter data acquired from relaxation tests, while the measured force response is represented by the *black curve*. *The green curve* corresponds to the best fit using reasonable mechanical parameters, clearly indicating that the model is not capable of predicting the reaction force in the case of constant compression rates (color figure online)

for all $x > 0$ and $i = 1, 2, 3$, which means that both the stiffness values and their derivatives with respect to the indentation depths must be nonnegative. The proposed nonlinear stiffness function is the following:

$$k_j(x) = K_j e^{\kappa_j x} \tag{14}$$

for $j = 1, 2, 3$. In this model, all of the three spring elements have the same nonlinear, exponential behavior, while the damping elements remain linear. This representation yields a total of 8 unknown parameters, providing a model that could be used in both relaxation and compression phases for reaction force estimation. The measurement data indicate that the force response is a convex curve in the case of constant compression rate indentation. As it is shown in Fig. 6 and as the result of the nature of (11), the linear Wiechert model always predicts a concave response curve. The proposed nonlinear model addresses this issue by introducing progressive stiffness and, therefore, logically would produce a better fit to the measurement data.

2.4 The proposed nonlinear mass–spring–damper model

Due to the nonlinear form of the model, no analytical expression for the force response can be obtained. Instead of using the MATLAB *cftool*, the *fminsearch* function was applied to find the optimal set of parameters [16]. The values of the individual mechanical parameters and combined root-mean-square error values are shown in Table 1. The curve fitting was carried out simultaneously on both datasets of 20 and 750 mm/min responses, and the combined error values were obtained as the sum of the individual errors for each curve, serving as the cost function for *fminsearch*. The estimated force responses, utilizing the parameters from Table 1, are shown in Figs. 7 and 8. In order to verify the parameters independently, a simulation was run on the nonlinear model with the obtained parameters, with the constant compression indentation rate of 100 mm/s. The nonlinear system can be represented by the following system of differential equations:

$$\begin{aligned}\dot{x}_0 &= v(t),\\ \dot{x}_1 &= \frac{1}{b_1}K_1(x_0 - x_1)e^{\kappa_1(x_0-x_1)},\\ \dot{x}_2 &= \frac{1}{b_2}K_2(x_0 - x_2)e^{\kappa_2(x_0-x_2)},\end{aligned} \tag{15}$$

where $v(t)$ is the surface deformation rate, x_0 denotes the position of an arbitrary point at the surface, while x_1 and x_2 represent two virtual points, connecting k_1–b_1 and k_2–b_2 elements, respectively. The system output is the reaction force, $F(t)$, calculated by

$$\begin{aligned}F(t) = {} & K_0 x_0 e^{\kappa_0 x_0} + K_1(x_0 - x_1)e^{\kappa_1(x_0-x_1)}\\ & + K_2(x_0 - x_2)e^{\kappa_2(x_0-x_2)}.\end{aligned} \tag{16}$$

3 Results

The simulation results were mapped on the experimental data, shown in Fig. 9. The average RMSE error, calculated separately with respect to each specimen, yielded $\varepsilon_{\mathrm{RMSE}} = 0.1748$ [N], which indicates that the model represents the investigated manipulation tasks very well. It was expected that the simulated curve gave lower force values than those of the measured, as the parameters were obtained partly by fitting the curve on the step-response. In the simulation, ideal step input was assumed, while, during the experiments, the maximum indentation speed was 750 mm/min. This lower-than-desired indentation speed yielded lower stiffness values due to the rapid relaxation during the compression phase. The effect can be observed in both Figs. 7 and 9.

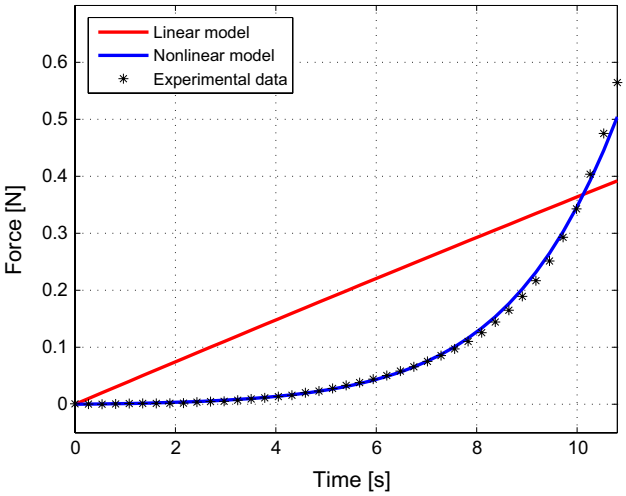

Fig. 7 Force response estimation curves, utilizing the parameter sets from Table 1, at the constant compression rate of 20 mm/s

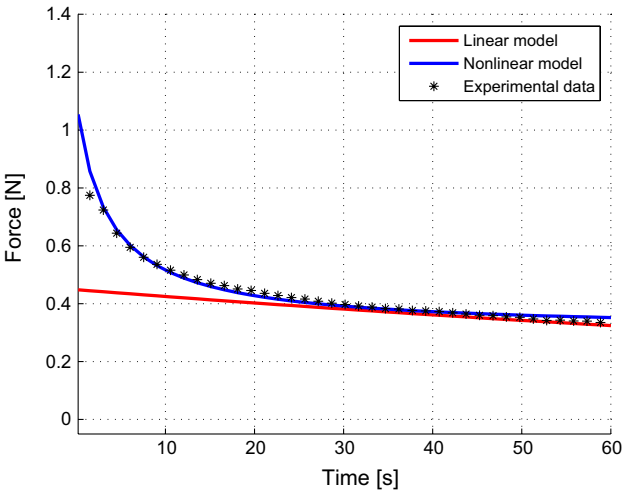

Fig. 8 Force response estimation curves, utilizing the parameter sets from Table 1, in the case of a step-like input, focusing on stress relaxation data

3.1 Model verification methods

In order to verify the approach proposed in Fig. 1, extended to the case of nonuniform surface deformation, additional palpation tests were carried out. Three specimens with the dimensions of 25 × 25 × 200 mm from the same beef liver were palpated with a sharp instrument, though not physically damaging the surface. Constant rate indentations were carried out at four different indentation rates (5, 10, 20 and 40 mm/s) at different points of the surface of each specimen, reaching 6 mm of indentation depth. The indenter used for the experiments was a 3D-printed piece that was mounted on the flat instrument used in the experiments at

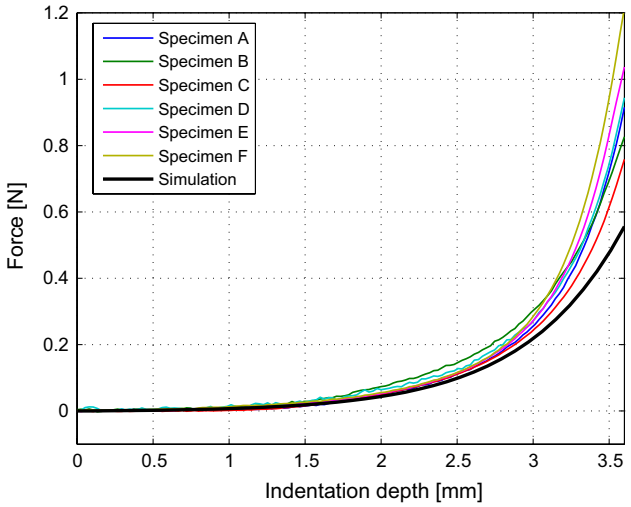

Fig. 9 Force response curves for constant compression rate indentation tests at 100 mm/min, showing the simulated response of the nonlinear model, using the parameters listed in Table 1

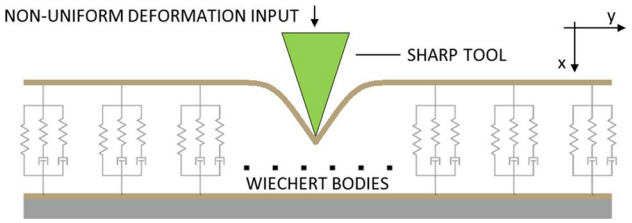

Fig. 10 The schematic figure of the nonuniform indentation tests

Table 2 Specific parameter values for the use of nonuniform surface deformation model verification

K_0^s(N/m^3)	K_1^s(N/m^3)	K_2^s(N/m^3)	b_1^s(N/m^3)
5075	1095	255	$127 \cdot 10^6$
b_2^s(N/m^3)	κ_0(m^{-1})	κ_1(m^{-1})	κ_2(m^{-1})
$1.1 \cdot 10^6$	909.9	1522	81.189

uniform deformation. At the tip, the indenter had a bevel angle of 30°, its length was 30 mm. It was assumed that the indenter created a line-like deformation input on the surfaces of the specimens, perpendicular to their longest dimensions. The schematic figure of the nonuniform indentation is shown in Fig. 10.

In order to estimate the reaction force, a few assumptions have been made prior to the verification:

- only uniaxial deformation is considered; therefore, all nonvertical forces are neglected in the calculations,
- it is assumed that the indentation only affects the liver structure in a certain ρ distance from the indentation point,
- the surface deformation shape is approximated as a quadratic function and is uniform along the width of the specimen.
- The reaction force is assumed to be the sum of the reaction of infinitely small elements on the tissue surface:

$$F(t) = \iint_{y,z} f(y,z,t)\mathrm{d}y\mathrm{d}z, \tag{17}$$

where $f(y, z, t)$ is the force response of a single infinitely small element at the surface point (y, z) at a given time t. $f(y, z, t)$ can be calculated by solving (16) for each surface element, using the unique deformation rate $v_{x,y}(t)$ of the element and utilizing *specific* stiffness and damping values shown in Table 2. These specific values were obtained by normalizing the appropriate parameters to the surface size of 1 m^2. The tissue surface was discretized using square-shaped elements $A_i = A_{y_i,z_i}$ with the edge length of 0.1 mm.

The corresponding deformation rate profiles, $v_i(t)$, were obtained as follows. The indentation tests were recorded by a video camera, fixed along the z-axis. Movements of 7 surface points were tracked by analyzing 12 video files frame-by-frame, at the time intervals of 1 s. The resolution of the picture was 1980 × 1080 pixels; the recordings were taken at 25 frames per second. An average deformation profile was calculated by processing the data manually. It was found that a quadratic function was a good approximation to the final deformation surface (after reaching the $x_d = 6$ mm indentation depth), assuming that the deformation surface is symmetrical to the axis of indentation. Furthermore, the doming effects were also neglected during the indentation. The effect of these assumptions is more relevant at the regions far from the indentation point, and due to the progressive spring characteristics in the model, these regions contribute very little to the overall force response. Utilizing the assumptions above, the deformation rate profile $v_i(t)$ can be obtained at each surface point A_i, provided by the following equation:

$$v(y,t) = \frac{v_{in}}{\rho^2}(|y| - \rho)^2, \tag{18}$$

indicating that in the case of constant indentation rate, each surface point is moving at a constant speed. Equation (16) was solved for each element, and the force response was obtained and summed using the velocity profiles according to (18).

3.2 Model verification results

Simulation results and the estimated force response for the 3rd specimen at 10 mm/min indentation rate are shown in

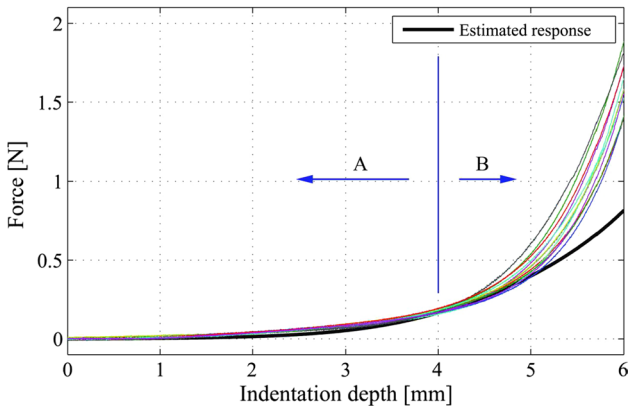

Fig. 11 Measurement results and estimated force response for the case of 10 mm/min indentation for nonuniform surface deformation. The model fits the experimental data very well in region A, while in region B this approach should be used with care

Fig. 11. The calculations were carried out on an Intel Core i5-3337U CPU with 8GB RAM; the simulation time was varying between approximately 0.5–1.5 s, depending on the indentation speed (length of the experiment). According to this performance, the method can be used in applications for semi-real-time force estimation. It is shown in Fig. 11 that the measured force response curves initially follow the estimated curve reasonably well, both qualitatively and quantitatively (region A). It can be observed that at the indentation depth of 4 mm, the slope of the measured curves increases rapidly, which is assumed to be due to the tension forces arising in the normal direction with respect to the indentation axis (region B). This is an expected behavior, indicating that at higher deformation levels, the 1 DoF approach of the problem should be handled with caution. This region will be investigated in depth in our future work. The RMSE values for each verification case were computed, with the results varying between $\varepsilon_{\mathrm{RMSE,min}} = 1.384$ and $\varepsilon_{\mathrm{RMSE,max}} = 2.8214$ N. The proposed soft tissue model can also be extended to more complex surface deformation functions. Given that the boundary conditions are well defined, one would find finite element modeling methods a useful tool for determining the surface deformation shape function [3].

4 Discussion

During our literature research on soft tissue models, we found that the verification of mass–spring–damper models is mostly limited to stress relaxation tests. This finding leads to a detailed study of these widely used linear models, pointing out that their applicability is very limited in practical use for robotic surgery applications. The proposed model addressed this issue by accounting for the progressive stiffness characteristics of soft tissues and was verified using uniaxial compression tests. Lateral tension forces were not taken into consideration in this approach, limiting usability in the case of sudden changes and steep slopes in the surface shape. Our future work includes taking lateral stretching into account, so that these effects can be compensated. In practice, this model could become a useful tool for creating virtual surgical simulators and to give a close estimation to the reaction forces during surgical interventions, enabling haptic feedback integration in model-based robot control systems. Based on the current results, future work includes the validation of the model on various soft tissue samples, real-time prediction of the reaction force using online deformation shape determination and extension of the model to more complex surface deformations, accounting for the lateral forces. Finally, the model could be integrated into virtual surgical simulators.

5 Conclusions

Rheological soft tissue models remain popular in medicine-related engineering applications, thanks to the simple modeling opportunities and reduced computational requirements they offer. Reaction force estimation and realistic real-time behavior modeling are some of the key advantages underlying this approach. If the surface deformation is known over time, the reaction force arising due to the tissue manipulation can be estimated, for which this paper presented a novel model and method. The model was verified on beef liver tissue samples, highlighting the advantages of the nonlinear Wiechert model compared to the widely (and in some cases, incorrectly) used linear models. The approach has been verified using both uniform and nonuniform surface deformation tests, yielding a good estimation of the reaction forces. In the author's opinion, these findings would serve as a major contribution to model-based design and control methods of modern medical applications, primarily in the field of surgical robotics.

References

1. Alkhouli N, Mansfield J, Green E, Bell J, Knight B, Liversedge N, Tham JC, Welbourn R, Shore AC, Kos K, Winlove CP (2013) The mechanical properties of human adipose tissues and their relationships to the structure and composition of the extracellular matrix. Am J Physiol Endocrinol Metab 305:1427–1435. doi:10.1152/ajpendo.00111.2013
2. Bao Y, Wu D, Yan Z, Du Z (2013) A new hybrid viscoelastic soft tissue model based on meshless method for haptic surgical simulation. Open Biomed Eng J 7:116–124. doi:10.2174/1874120701307010116
3. Buijs JOP, Hansen HHG, Lopata RGP, Korte CLD, Misra S (2011) Predicting target displacements using ultrasound

elastography and finite element modeling. IEEE Trans Biomed Eng 58:3143–3155. doi:10.1109/TBME.2011.2164917
4. Constantinesco A, Schwerdt H, Chambron J (1981) Testing device to determine the dynamic rheological properties of soft tissues in biaxial elongation. Med Biol Eng Comput 19:129–134. doi:10.1007/BF02442705
5. Famaey N, Sloten JV (2008) Soft tissue modelling for applications in virtual surgery and surgical robotics. Comput Methods Biomech Biomed Eng 11:351–366. doi:10.1080/10255840802020412
6. Haidegger T, Kovacs L, Precup RE, Benyo B, Benyo Z, Preitl S (2012) Simulation and control for telerobots in space medicine. Acta Astronaut 81(1):390–402
7. Hoeckelmann M, Rudas IJ, Fiorini P, Kirchner F, Haidegger T (2015) Current capabilities and development potential in surgical robotics. Int J Adv Robot Syst 12(61):1–39. doi:10.5772/60133
8. Leong F (2009) Modelling and analysis of a new integrated radiofrequency ablation and division device, M.Sc. Thesis, National University of Singapore
9. Leong F, Huang WH, Chui CK (2013) Modeling and analysis of coagulated liver tissue and its interaction with a scalpel blade. Med Biol Eng Comput 51:687–695. doi:10.1007/s11517-013-1038-5
10. Li M, Konstantinova J, Secco EL, Jiang A, Liu H, Nanayakkara T, Seneviratne LD, Dasgupta P, Althoefer K, Wurdemann HA (2015) Using visual cues to enhance haptic feedback for palpation on virtual model of soft tissue. Med Biol Eng Comput. doi:10.1007/s11517-015-1309-4
11. Machiraju C, Phan AV, Pearsall AW, Madanagopal S (2006) Viscoelastic studies of human subscapularis tendon: relaxation test and a Wiechert model. Compu Methods Programs Biomed 83:29–33. doi:10.1016/j.cmpb.2006.05.004
12. Maurel W, Thalmann PD, Wu Y, Thalmann PNM (1998) Biomechanical models for soft tissue simulation. Esprit basic research series. Springer, Berlin
13. Parker KJ (2014) A microchannel flow model for soft tissue elasticity. Phys Med Biol 59:4443. doi:10.1088/0031-9155/59/15/4443
14. Pelyhe L, Nagy P (2014) Relative visibility of the diagnostic catheter. Acta Polytech Hung 11(10):79–95
15. Rosen J, Brown JD, De S, Sinanan M, Hannaford B (2008) Biomechanical properties of abdominal organs in vivo and postmortem under compression loads. J Biomech Eng 130(2):021020. doi:10.1115/1.2898712
16. Takacs A, Galambos P, Rudas IJ, Haidegger T (2015). Nonlinear soft tissue models and force control for medical cyber-physical systems. In: IEEE international conference on systems, man and cybernetics (SMC2015), Hong Kong, Paper 10457
17. Takacs A, Jordan S, Precup RE, Kovacs L, Tar J, Rudas IJ, Haidegger T (2014) Review of tool-tissue interaction models for robotic surgery applications, In: 2014 IEEE 12th International symposium on machine intelligence and informatics (SAMI), pp 339–344. doi:10.1109/SAMI.2014.6822435
18. Troyer KL, Shetye SS, Puttlitz CM (2012) Experimental characterization and finite element implementation of soft tissue nonlinear viscoelasticity. J Biomech Eng 134(11):114501. doi:10.1115/1.4007630
19. Wang X, Schoen JA, Rentschler ME (2013) A quantitative comparison of soft tissue compressive viscoelastic model accuracy. J Mech Behav Biomed Mater 20:126–136. doi:10.1016/j.jmbbm.2013.01.007
20. Wang Z, Hirai S (2010) Modeling and parameter estimation of rheological objects for simultaneous reproduction of force and deformation. In: 1st international conference on applied bionics and biomechanics, Venice
21. Yamamoto T (2011) Applying tissue models in teleoperated robot-assisted surgery. Ph.D. Thesis, The Johns Hopkins University

Árpád Takács received his M.Sc. degree from the Budapest University of Technology in Mechanical Engineering. He is currently doing his Ph.D. studies in surgical robotics at Óbuda University.

Imre J. Rudas is a D.Sc. of the Hungarian Academy of Sciences, formal President of Óbuda University. Fellow IEEE and Distinguished Lecturer, holder of the Order of Merit of the Hungarian Republic.

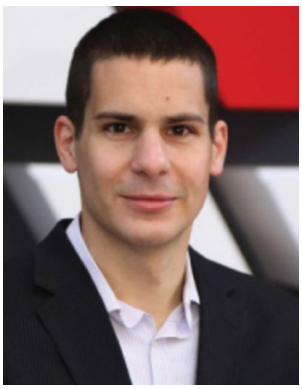

Tamás Haidegger is an adjunct professor at Óbuda University, deputy director of the ABC-iRob and research area manager at the Austrian Center of Medical Innovation and Technology (ACMIT).